Huang, Bingkun; Yang, Shimi; Lund, Peter D.

Optimizing the shape of PCM container to enhance the melting process

Published in:
Oxford Open Energy

DOI:
10.1093/ooenergy/oiab006

Published: 10/01/2022

Document Version
Publisher's PDF, also known as Version of record

Oxford Open Energy, 2022, 1–10
https://doi.org/10.1093/ooenergy/oiab006
Research Article

Optimizing the shape of PCM container to enhance the melting process

Bingkun Huang[1], Shimi Yang[1], Jun Wang[1,*] and Peter D. Lund[1,2,*]

[1]Jiangsu Provincial Key Laboratory of Solar Energy Science and Technology, School of Energy and Environment, Southeast University, No. 2 Si Pai Lou, Nanjing 210096, P.R. of China
[2]School of Science, Aalto University, P.O. Box 15100, FI-00076 Espoo, Finland
*Correspondence address. Jiangsu Provincial Key Laboratory of Solar Energy Science and Technology, Southeast University School of Energy and Environment, Nanjing 210096, P.R. of China. E-mail: 101010980@seu.edu.cn, lund@aalto.fi

Abstract

The shape of container influences natural convection inside a latent heat storage with a phase change material (PCM). Often, the geometrical design of a PCM container is based on empirical observations. To enhance convection and melting of the PCM, authors propose here new design guidelines for an improved container. Using the so-called Co-factor method as the optimized basis, which is defined as the vector product of the velocity and temperature gradient, the new design method strives to raise the velocity of natural convection in liquid PCM, increase the amount of PCM in the direction of the convective flow, and reduce the amount of PCM far from the heating surface. Following these guidelines and Co-factor, an optimized PCM container with an elongated and curved shape is proposed and compared with a rectangular container. Numerical simulations indicated that the total melting time of the PCM in the optimized container could be reduced by more than 20% compared with the rectangular one. The higher natural convection velocity and the better use of it to melt the PCM in the optimized container space attributed to the better performance than that in rectangular container. The results can be used to design more effective PCM storage systems.

Keywords: heat transfer analysis, natural convection, enhance convection and melting, PCM container, latent heat storage

INTRODUCTION

Thermal storage has been identified as an important technology to match unbalanced heat demand and supply and in connection with renewable energy [1–8]. Heat can be stored in three different ways: sensible heat, latent heat and thermo-chemical heat storage. Latent heat thermal storage makes use of the heat of transformation in phase change materials (PCMs), e.g. between a solid and liquid phase [9]. It is considered a promising storage option due to a high storage density and operation at close to isothermal conditions [10, 11]. A latent heat storage system comprises the PCMs, a container and heat transfer devices [12]. These systems have been subject to intensive research, e.g. on new PCMs, improving thermal conductivity of PCM, microencapsulation of PCM [13], enhancing heat transfer in PCM [14] and optimization of the system structure [15].

The container of the latent heat storage not only provides a confinement of the PCM but also affects the heat transfer inside the storage and hence its performance [16]. Rectangular [17] and cylindrical [18] containers and sphere [19] capsules are commonly used with PCM. In addition to the influence of container shape on PCM melting process, natural convection also plays an important role in PCM melting. Numerical and experimental studies on the melting process showed that natural convection enhances the melting process and emphasized the use of conduction–convection coupled heat transfer models [20, 21]. Actually, several studies have focused to enhance PCM melting by natural convection [22–24]. In fact, the mode of natural convection is affected by a variety of external conditions, such as heating location [25] and container shape [26, 27]. Many scholars have studied the melting process of PCM in different container shapes and the role of natural convection [16, 28]. Vogel *et al.* [29] investigated the melting process in flat plate; the heat transfer is enhanced by greater widths and smaller heights of enclosure. Shin *et al.* [28] reported that elliptical capsules enhanced the Nusselt number of the PCM by five times compared with the spherical capsules. Although the melting process of PCM in different shapes of containers affected by natural convection has been widely studied, due to the diversity of container shapes and boundary conditions, the understanding of melting cannot be extended to the optimization of other container shapes.

Received: September 10, 2021. **Revised:** November 9, 2021. **Accepted:** December 17, 2021

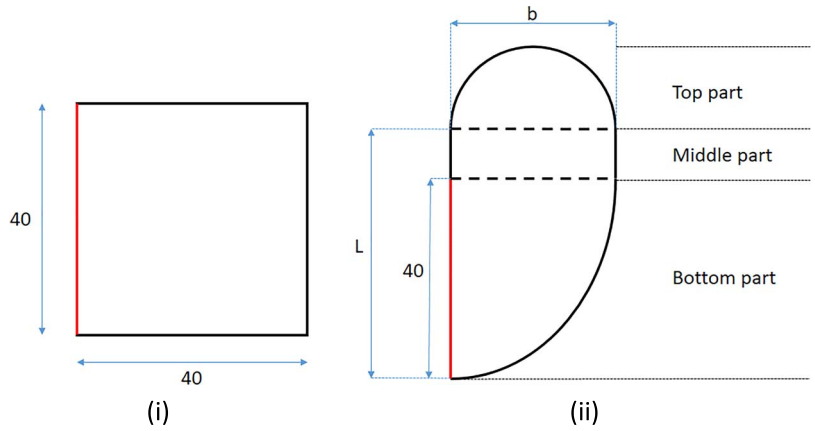

Fig. 1. Physical model of a rectangular container (i) and the new design of container (ii)

Rectangular container is a common PCM container model, which can come from the square container or symmetrical section plane of shell and tube [16, 26, 29]. In the rectangular container, one side is often used as the heating surface and the other surfaces are adiabatic [30]. A previous work on rectangular containers has shown that controlling the heat flux importantly affects the heat transfer and fusion velocity in PCM [31, 32]. In addition to the above changes, tilting the container at a certain angle can also enhance the heat transfer [33–35], but this can be regarded as a double change of the position of the heating surface and the container shape.

To sum up, there are many ways to strengthen the heat transfer process by changing the shape, but their conclusions are not generalizable, the optimization direction for the shape of PCM container is not clear, and it is difficult to be used in the optimization of other container shapes. Combined with the previous research on natural convection [25, 36], the authors believe that the natural convection flow is affected by the heating position and the shape of the container and the velocity direction of natural convection plays an important role in the PCM melting process. Therefore, when the heating surface is unchanged, the optimization mode of PCM container is given according to the natural convection flow pattern. This conclusion has wide applicability in the heat storage system with natural convection and can be optimized according to the original shape.

In this paper, the authors take the common rectangular container as the prototype, optimize the rectangular container under the condition of keeping the total volume unchanged and make a detailed analysis of the results according to the previous research conclusions to reveal what factors cause the 'enhanced heat transfer'.

METHOD OF OPTIMIZING PCM CONTAINER

Design guidelines

As a starting point for the design of a PCM container, the authors prioritize enhancing the natural convection in improving the thermal performance. Traditional engineering aspects such as mechanical strength and isolation of the container are not considered here. Authors of the previous work [36] show that the vector product of the velocity and thermal gradient vectors $\vec{U} \cdot \vec{\nabla T}$ ($\vec{U}$ = velocity, $\vec{\nabla T}$= temperature gradient) is a main driving force of melting in the convection-regime of the temperature boundary layer. Denoting $Co = \vec{U} \cdot \vec{\nabla T}$, and naming this as the Co-factor, when $Co > 0$ it promotes melting. This model gives a clear and quantitative explanation for the problem of melting interface movement affected by natural convection, as well as that increasing the heating temperature and changing only the shape of the heat storage unit can greatly enhance the heat storage rate in this study.

Based on the above, the following design guidelines of PCM container are proposed:

- increase velocity of natural convection or reduce attenuation of convection in liquid PCM;
- increase amount of PCM in direction of convective flow;
- reduce amount of PCM far away from heating surface where natural convection is weak.

Combining the above factor with the fluid flow characteristics (convection by buoyancy is upwards; convection flows along container wall and solid–liquid interface; convection flow is a closed loop), the PCM melting process in the container can be predicted and the effect of the container shape can be judged. These will be discussed in the following.

Container shape

In the next, the authors proposed a new container shape outgoing from earlier observations from literature with different dimensions [16] and optimized the rectangular container. The authors extend the length above the heating wall so that more PCM is located in the convection direction and convert the right angle turning into a smooth curve to reduce the convective loss and thus the PCM away from heating wall will be reduced due to this arrangement. For comparison, a rectangular container is also analyzed. All containers have the same

Table 1. Shape parameters of the new containers

L(mm)	40	45	50	55	60
b(mm)	35.4	32.6	30.1	27.9	26.0

PCM volume. The rectangular and the new containers shown in 2D in Fig. 1 are all heated over a 40-mm length on the left vertical side and the remaining surfaces are well insulated. The geometric parameter values are given in Table 1. Therefore, the top of the new containers is designed semicircular and the bottom part is a quarter ellipse in order to ensure smooth wall curve; the middle part is rectangular (there is no middle part when L = 40 mm) for longer lengthening but will not lengthen the wall indefinitely. Their area can be calculated by the following formula; the three parts are the area of semicircle (top part), rectangular (middle part) and quarter ellipse (bottom part).

$$S_{area} = \frac{1}{2}\frac{\pi b^2}{4} + b\,(L - 40) + \frac{1}{4}40b\pi$$

Thermal model of the PCM

In the numerical model of the PCM storage, the flow is considered unsteady, laminar, incompressible and 2D. The viscous dissipation term is neglected. The viscous incompressible flow and the temperature distribution are solved using the Navier–Stokes and thermal energy equations, respectively. The continuity, momentum and thermal energy equations can be expressed as follows [37]:

Continuity:

$$\frac{\partial \rho}{\partial t} + \nabla\left(\rho \vec{U}\right) = 0, \tag{1}$$

where ρ is the density of the PCM, $\vec{U}$ is the velocity.

Momentum:

$$\frac{\partial}{\partial t}\left(\rho \vec{U}\right) + \nabla \cdot \left(\rho \vec{U}\,\vec{U}\right) = -\nabla P + \rho \vec{g} + \nabla \cdot \tau + \vec{F}, \tag{2}$$

where P is the static pressure, τ is the stress tensor and $\vec{g}$ is acceleration of gravity and $\vec{F}$ is the external body forces, which is equal to 0 in this article.

Thermal energy:

$$\frac{\partial (\rho H)}{\partial t} + \nabla \cdot \left(\rho \vec{U} H\right) = \nabla \cdot (K \nabla T) + S, \tag{3}$$

where H is enthalpy, T is the temperature, k is the thermal conductivity of the PCM and S is the volumetric heat source term, which is equal to zero here. The enthalpy H of the PCM is computed as the sum of the sensible enthalpy h and the latent heat ΔH, where the sensible enthalpy h is

$$h = h_{ref} + \int_{T_{ref}}^{T} c_p dT \tag{4}$$

and h_{ref} is reference enthalpy, T_{ref} is the reference temperature, c_p is the specific heat at constant pressure.

The latent heat ΔH is

$$\Delta H = \beta La, \tag{5}$$

where La is the latent heat, β is the liquid fraction defined as

$$\beta = 0, \quad \text{if } T < T_{solid} \tag{6}$$

$$\beta = 1, \quad \text{if } T > T_{liquid} \tag{7}$$

$$\beta = \frac{T - T_{solid}}{T_{liquid} - T_{solid}}, \quad \text{if } T_{solid} < T < T_{liquid} \tag{8}$$

The above equations are numerically solved by the ANSYS FLUENT 16.0 model [38]. The SIMPLE method for the pressure–velocity coupling is used in order to solve the momentum and energy equations, and the PRESTO scheme is adopted for the pressure correction equation. The under-relaxation factors for the pressure, velocity components, liquid fraction and thermal energy are 0.3, 0.2, 0.9 and 1 [23], respectively. A residual target of 10^{-5} is used for the continuity, momentum and energy equations. N-eicosane is selected as PCM due to it has been widely used in research [23]. The thermal properties are shown in Table 2.

Table 2. Thermophysical properties of N-eicosane [23]

Properties	Values
Melting temperature	36 (35–37) °C
Density	770 kg/m^3
Kinematic viscosity	5×10^{-6} m^2/s
Specific heat	2460 J/kg K
Thermal conductivity	0.151 W/m K
Latent heat	247.6 kJ/kg
Thermal expansion coefficient	0.0009 K^{-1}

In time t = 0, the temperature of the PCM in the containers is set to 308.15 K (T_0), and the heating wall is set to a constant temperature of 350.15 K (T_h).

Validation of the model

As part of the model validation, the authors first ensured the independency of the numerical solution from the grid. For the new container with L = 40 mm, three meshes were considered and the corresponding evolution of the liquid fraction was tracked and shown in Fig. 2. A grid size with 6591 elements was selected also taking the required computer run time into account. Time step (dt) for numerical calculation was also checked illustrated in Fig. 3 indicating that there is no difference between

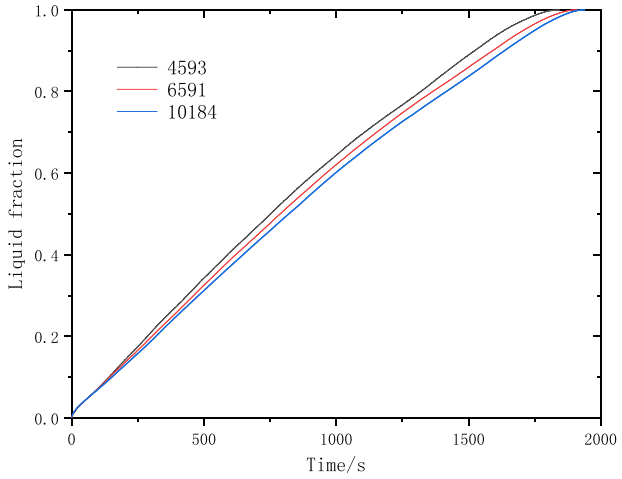

Fig. 2. Testing the effect of grid size in the numerical simulations

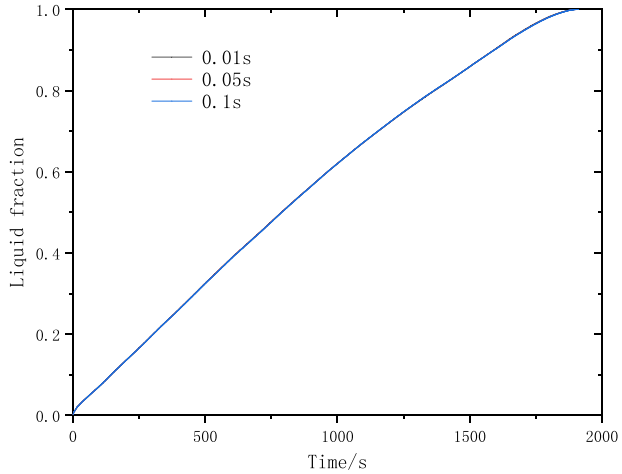

Fig. 3. Testing the time step dependence in the numerical simulations

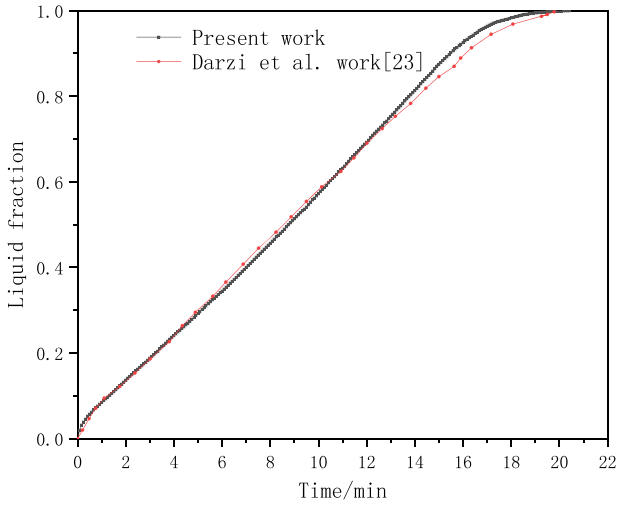

Fig. 4. Validation of the present model with Darzi *et al.* [23] (array 3) work

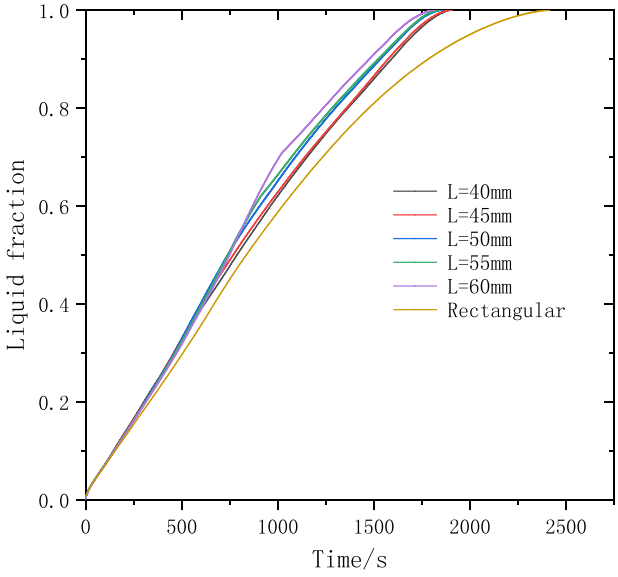

Fig. 5. Change of liquid fraction in different containers versus time

the three time steps (dt = 0.01, dt = 0.05, dt = 0.1). The computing time increased with shorter time steps but more iterations are needed with the longer time steps, for which reason the authors chose 0.05 s as the time step in the numerical simulation.

To validate the present simulation model, a comparison with pure N-eicosane melt in a concentric circular annulus is performed with array 3 in [23] similar to [39]. Figure 4 shows a good agreement between the present simulation and [23].

RESULTS AND DISCUSSION

Comparison of rectangular and new containers

Figure 5 shows the change of the liquid fraction with time for the different geometries of the container. The time required for complete melting of the PCM is given in Table 3. The results show that the time needed for complete melting of the PCM is shorter with the new containers than with the rectangular one. The time reduction improves with the length: for L = 40 mm, L = 45 mm, L = 50 mm, L = 55 mm and L = 60 mm, the time is reduced by 20.9%, 21.1%, 23.0%, 23.7% and 25.1%, respectively. It should be noted that in the new container with L = 60, the liquid fraction has a significant turning point at 1010s and the turning also appears with L = 55 in the new container. The specific reasons for this are discussed in Advantages of the new containers based on the Co-factor.

The melting process including the velocity vectors are shown in Fig. 6. The magnitude of speed is set to the same during post-processing to compare the velocity in the different case. The velocity in the new designs is higher than in the rectangular container from the beginning to the end of the melting process, especially above the vertical heating surface. The velocity in the rectangular container needs to go through a right angle turn and this causes a main loss in the turning. Similar velocity distribution has been found in [26]. The melting interface in the containers shows that the melting rate of the solid phase PCM is faster in the direction of the velocity. More solid PCM is placed in the direction of the natural convection velocity in the new type of containers, leading

Table 3. Complete melting time of PCM in different container shapes

Container shape	Rectangular	New design (L = 40 mm)	New design (L = 45 mm)	New design (L = 50 mm)	New design (L = 55 mm)	New design (L = 60 mm)
Complete melting time (s)	2415	1910	1906	1860	1843	1813

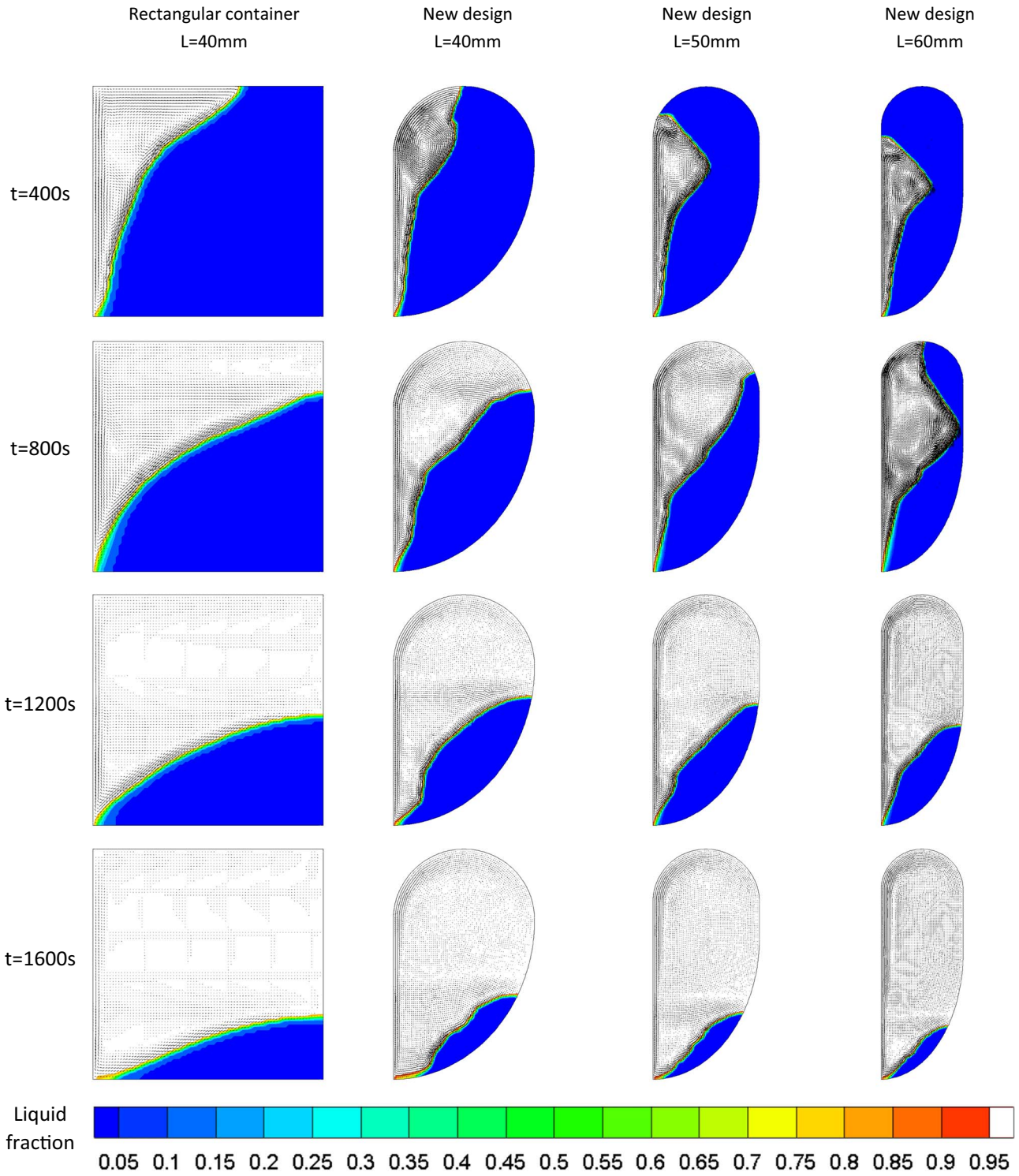

Fig. 6. Melting interface and velocity vectors for the different containers

to faster melting rate. It is worth noting that in a later stage of the melting process, the melting rate of the PCM is slower when it is not in the direction of the velocity, which is well observed with increasing of L. When the faster part is melted, the melting rate will change significantly and that is why there is an obvious turning point

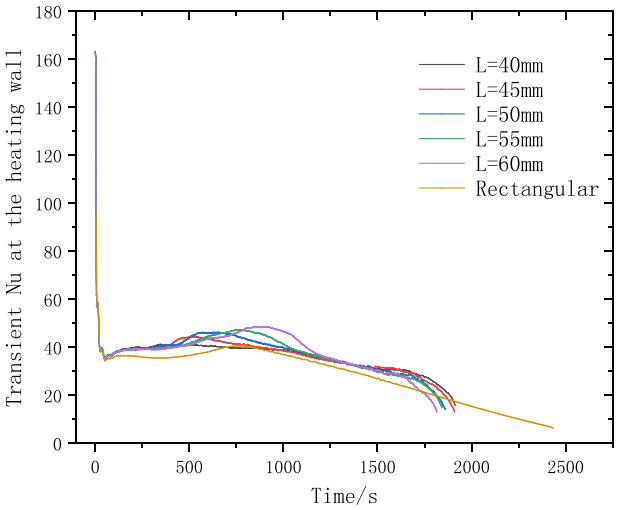

Fig. 7. Comparison of transient Nu at the heating wall for rectangular container and new designed container

when L = 60 mm in Fig. 5. This phenomenon is caused by the difference of PCM melting rate at different locations. Above the heating surface, the melting rate of PCM is faster than that below, and the melting rate is the sum of the melting rates above and below. However, after the PCM above melts completely, there is no part of the faster melting rate, so the melting rate turns suddenly. These phenomena also correspond to the reduction of Nu in Fig. 7.

To analyze the heat transfer process further, a transient Nusselt number (*Nu*) on the heating wall is defined as follows:

$$Nu(t) = \frac{h(t)l}{k},$$

(9)where h(t) is the average heat transfer coefficient at the heating wall, k is the thermal conductivity of the PCM and l is characteristic length of the container (=40 mm in this paper). The heat transfer coefficient can further be defined as

$$h(t) = \frac{Q(t)}{A\,(T_h - T_m)},$$

(10)where Q(t) is the heat transferred from the heating wall to PCM per unit time interval, A is the area of the heating wall, T_h is the heating temperature, T_m is the melting temperature.

Nu(t) for the different containers is shown in Fig. 7. The trend of the six curves over time is consistent and can be divided into three stages over time. First, the Nusselt number drops quickly, then it rises slightly, and finally, it decreases until the PCM melts completely. Heat conduction dominates melting in the early stage, but heat convection gradually starts to dominate the heat transfer. Compared with the rectangular container, the *Nu* of the new type of containers is higher in the convection-dominated regime except for the new container with L = 40 mm, but just for a short period of time. The higher Nusselt number explains why the PCM in the new containers melts faster than in the rectangular one. In addition, the maximum value of *Nu* increases and the duration of the second stage is prolonged with increasing L explaining the shorter time needed for complete melting with increasing L.

Advantages of the new containers based on the Co-factor

To better understand the role of natural convection in the melting process, further analysis on influencing factors was made. From the previous sector, it can be found that the liquid fraction, melting interface and Nusselt number are closely related to melting but do not provide adequate information on the role of natural convection. Natural convection has two key parameters: speed and direction, which cannot be reflected in Nu and liquid rate, but Co is the dot product value, including these two parameters. Therefore, the Co-factor will be used next for a more detailed analysis of the natural convection. According to the Co-theory [36], the PCM melting rate can be improved through the following measures: increasing the flow rate or the temperature gradient, reducing the angle between the velocity and the direction of the temperature gradient and striving for placing the maximum velocity and the maximum temperature gradient in the same position.

First, the melting process is analyzed based on the velocity (v) of natural convection. Three different velocity points are defined: the maximum velocity in the liquid zone (v_{max}), the velocity at maximum Co (v_{Co}) and the velocity in the direction of the temperature gradient at maximum Co (v_{TG}). Also, the following hold: $v_{TG} \le v_{Co} \le v_{max}$. Figure 8a–f illustrates these velocities for the different containers. Coincide of v_{Co} and v_{max} means that the position of the maximum Co coincides with that of the maximum velocity; it implies whether natural convection is better used for melting. The v_{TG} is an important part of the Co-factor, which indicates how much natural convection contributes to the melting at this location. From Fig. 8a–f, it can be seen that the v_{TG} has a low coincides with v_{Co} at maximum Co position, which means all their natural convection are not fully utilization for promoting melting. The magnitude of v_{TG} and v_{Co} are clearly separated in time, which indicates that the PCM in the direction of the velocity flow has completely melted; it can be verified with the melting process. Melting rate will become lower because poor utilization of velocity and it can also verified by integral analysis in next paragraph. The maximum velocity in the rectangular container and both coincides of velocity are lower than that of the new containers explaining the slower melting rate in the rectangular container. With increase of L in the new containers, the duration of coincide time of v_{Co} and v_{max} increases and the time for complete melting of the PCM decreases. The same kind of result has been mentioned [16]. When L is equal to 55 and 60 mm, the v_{max} and v_{TG} have an obvious turning

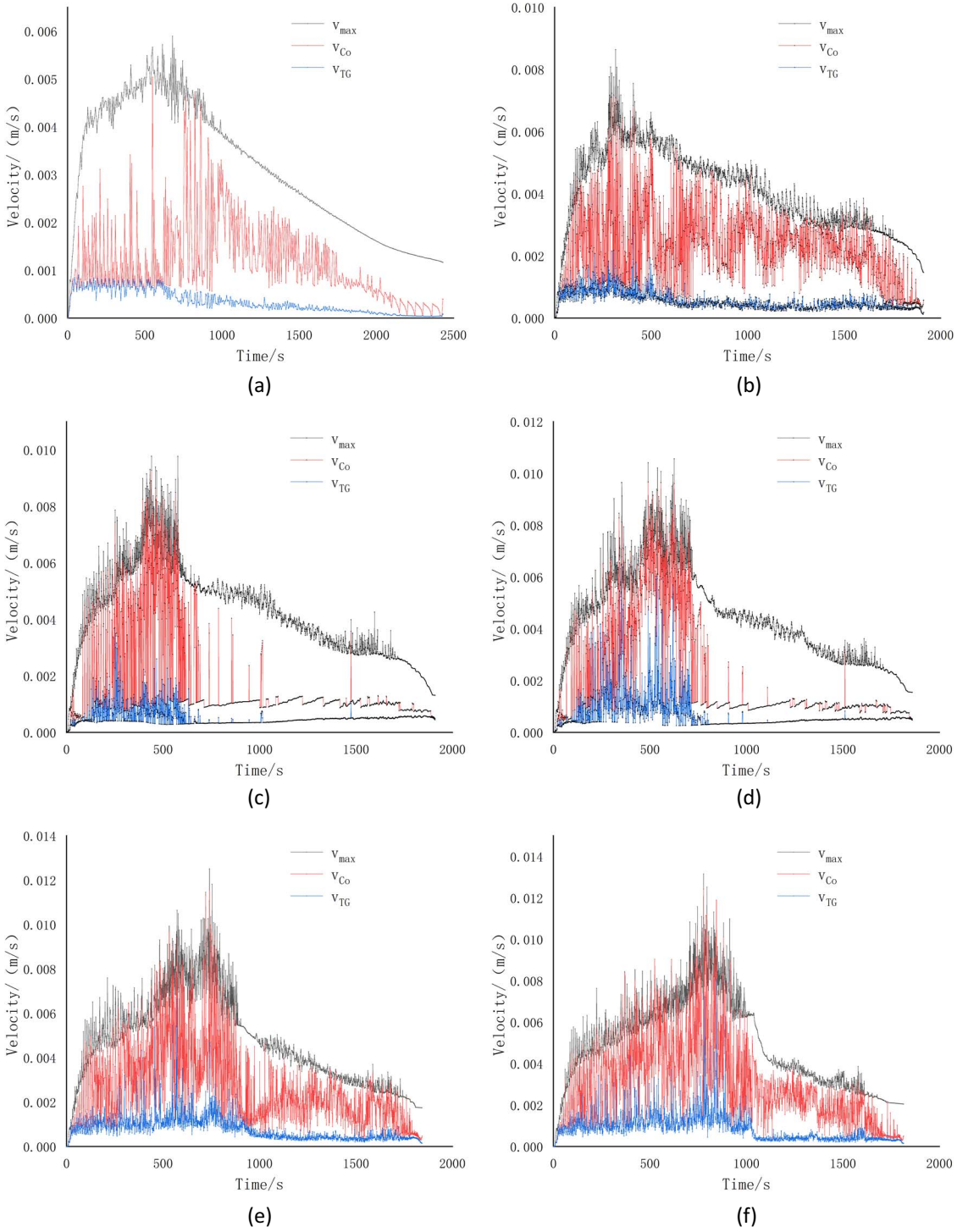

Fig. 8. Three velocities in the different containers (a) rectangular, new design (b) L = 40 mm, (c) L = 45 mm, (d) L = 50 mm, (e) L = 55 mm, (f) L = 60 mm

point, which reflects to the liquid fraction having also a turning point.

Next, an integral analysis was performed. As $Co > 0$ in the temperature boundary layer is regarded as the driving force of melting in the convection-regime; then the integral of Co for values $Co > 0$ on the surface represent the melting rate of PCM. The melting rate of PCM is expressed by the change rate of liquid fraction in a certain time. The melting rate and the integrals of Co are shown in Fig. 9a–f to illustrate this relationship. In the simulation, a time step of 1 s is used for the new containers and 5 s for the rectangular container. It should be noted that the integral of Co is taken over the whole surface, so it is slightly larger than that in the temperature boundary layer. The mixing of cold and hot fluids may exist outside the boundary layer where

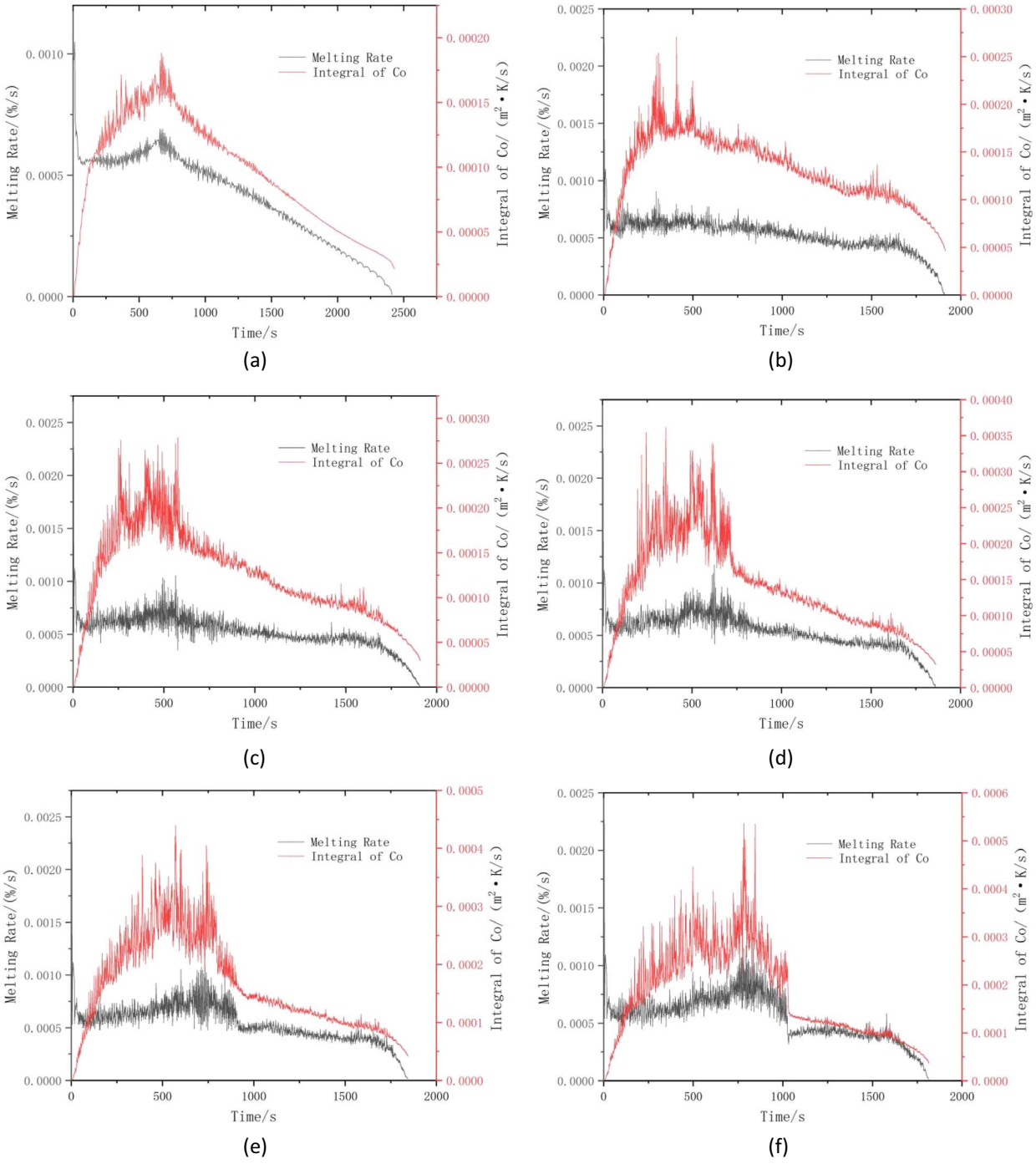

Fig. 9. Melting rate and integral of Co in the different containers (a) rectangular, new design (b) L = 40 mm, (c) L = 45 mm, (d) L = 50 mm, (e) L = 55 mm, (f) L = 60 mm

Co factor is also available. From Fig. 9a–f, the melting rate and integral value have similar trends, except for the initial stage, in which the melting mainly depends on heat conduction. The melting time of the PCM by heat conduction is about 250 s, and the subsequent PCM melting mainly depends on the convection heat transfer. Increasing L increases the maximum value of the integral and the higher value exists for a longer time. When L is equal to 55 and 60 mm, the integral value suddenly decreases at a certain time point, which leads to the turning point of the liquid fraction. Hence, the change of the integral value is the reason for the change of melting rate.

Summarizing, through the above analyses of the container design, it can be concluded that natural convection is better utilized in the new design of the containers. Moreover, the proposed method of velocity and integral analysis can also be used to analyze the natural convection in other PCM storage systems as these methods are not limited by the shape of the PCM container.

CONCLUSIONS

To enhance convection and melting in PCM, new design guidelines for an improved container have been proposed in this paper. Using the so-called Co-factor method for the design, a novel PCM container with an elongated and curved shape is proposed and compared with a rectangular container. Numerical simulations were conducted and the results indicate that a higher natural convection velocity and a better melting process of the PCM were achieved.

The results indicate that three factors in particular should be considered for making full use of natural convection resulting in quicker melting: raise the velocity of natural convection or reduce the attenuation of convection in liquid PCM; make more PCM available in the direction of convection flow; and reduce the amount of PCM far from the heating surface where the natural convection is weak.

New PCM containers based on the guidelines were proposed and compared with a standard rectangular container. Velocity analysis and integral analysis were employed for the comparison to verify the change of natural convection in the container. The melting time of the new containers with an elongated and curved shape is decreased by 20–25%, the higher value linked to an increased length of the surface.

The design method proposed here is independent of container geometry and it can be used for existing containers and optimize their shape, or to study the effects of different heat transfer enhancing measures such as fins, among others by velocity analysis and integral analysis.

FUNDING

This study was supported by the 'Fundamental Research Funds for the Central Universities' (2242021k30028) and was partially supported by Aalto University.

CONFLICT OF INTEREST

None declared.

AUTHORS' CONTRIBUTIONS

B.H.: methodology, conceptualization, validation, writing (original draft). S.Y.: methodology, formal analysis, writing (review and editing). J.W.: resources, project administration. P.D.L.: original editing.

References

1. Hasan A, Sayigh AA. Some fatty-acids as phase-change thermal-energy storage materials. *Renew Energy*. 1994;**4**:69–76
2. Ibrahim M, Sokolov P, Kerslake T *et al.* Experimental and computational investigations of phase change thermal energy storage canisters. *J Sol Energy Eng*. 2000;**122**:176–82
3. Bonadies MF, Ricklick M, Kapat JS *Optimization of a Phase Change Thermal Storage Unit*. New York: American Society of Mechanical Engineers, 2010
4. Siahpush A, O'Brien J, Crepeau J *et al. Scale analysis and experimental results of a sollid/liquid phase-change thermal energy storage system*. New York: American Society of Mechanical Engineers, 2015
5. Fleming E, Wen SY, Shi L *et al.* Experimental and theoretical analysis of an aluminum foam enhanced phase change thermal storage unit. *Int J Heat Mass Transf*. 2015;**82**:273–81
6. Xiao D, Qu YY, Hu SC *et al.* Study on the phase change thermal storage performance of palmitic acid/carbon nanotubes composites. *Compos Part A Appl Sci Manuf*. 2015;**77**:50–5
7. Liu L, Fan XQ, Zhang Y *et al.* Novel bio-based phase change materials with high enthalpy for thermal energy storage. *Appl Energy*. 2020;**268**:114979
8. Wei HT, Wang CP, Yang SY *et al.* Novel core/void/shell composite phase change materials for high temperature thermal energy storage. *Chem Eng J*. 2020;**391**:123539
9. Dhaidan NS, Khodadadi JM. Melting and convection of phase change materials in different shape containers: a review. *Renew Sust Energ Rev*. 2015;**43**:449–77
10. Waqas A, Ud DZ. Phase change material (PCM) storage for free cooling of buildings—a review. *Renew Sust Energ Rev*. 2013;**18**: 607–25
11. Ismail KAR, Alves CLF, Modesto MS. Numerical and experimental study on the solidification of PCM around a vertical axially finned isothermal cylinder. *Appl Therm Eng*. 2001;**21**:53–77
12. Kamkari B, Shokouhmand H. Experimental investigation of phase change material melting in rectangular enclosures with horizontal partial fins. *Int J Heat Mass Transf*. 2014;**78**:839–51
13. Jamekhorshid A, Sadrameli SM, Farid M. A review of microencapsulation methods of phase change materials (PCMs) as a thermal energy storage (TES) medium. *Renew Sust Energ Rev*. 2014;**31**:531–42
14. Zhang C, Yu M, Fan Y *et al.* Numerical study on heat transfer enhancement of PCM using three combined methods based on heat pipe. *Energy*. 2020;**195**:116809
15. Xie J, Lee HM, Xiang J. Numerical study of thermally optimized metal structures in a phase change material (PCM) enclosure. *Appl Therm Eng*. 2019;**148**:825–37
16. Barletta A, Nobile E, Pinto F *et al.* Natural convection in a 2D-cavity with vertical isothermal walls: cross-validation of two numerical solutions. *Int J Therm Sci*. 2006;**45**:917–22
17. Ji C, Qin Z, Low Z *et al.* Non-uniform heat transfer suppression to enhance PCM melting by angled fins. *Appl Therm Eng*. 2018;**129**: 269–79
18. Pourakabar A, Rabienataj Darzi AA. Enhancement of phase change rate of PCM in cylindrical thermal energy storage. *Appl Therm Eng*. 2019;**150**:132–42
19. Nazzi Ehms JH, De Césaro OR, Oliveira Rocha LA *et al.* Theoretical and numerical analysis on phase change materials (PCM): a case study of the solidification process of erythritol in spheres. *Int J Heat Mass Transf*. 2018;**119**:523–32
20. Hamdan MA, Al-Hinti I. Analysis of heat transfer during the melting of a phase-change material. *Appl Therm Eng*. 2004;**24**: 1935–44
21. Yanxia D, Yanping Y, Daiyong J *et al.* Experimental investigation on melting characteristics of ethanolamine-water binary mixture used as PCM. *Int J Heat Mass Transf*. 2007;**34**:1056–63
22. Zeng RL, Wang X, Chen BJ *et al.* Heat transfer characteristics of microencapsulated phase change material slurry in laminar flow under constant heat flux. *Appl Energy*. 2009;**86**:2661–70
23. Darzi AR, Farhadi M, Sedighi K. Numerical study of melting inside concentric and eccentric horizontal annulus. *Appl Math Model*. 2012;**36**:4080–6

24. Ezan MA, Erek A, Dincer I. A study on the importance of natural convection during solidification in rectangular geometry. *J Heat Transf-Trans ASME*. 2011;**133**:9
25. Yang S, Huang B, Wang J, Lund PD. Characteristics of natural convection in n-eicosane in a square cavity with discrete heat source. *Case Stud Therm Eng*. 2021;**27**:101245
26. El Omari K, Kousksou T, Le Guer Y. Impact of shape of container on natural convection and melting inside enclosures used for passive cooling of electronic devices. *Appl Therm Eng*. 2011;**31**: 3022–35
27. Patel JR, Joshi V, Rathod MK. Thermal performance investigations of the melting and solidification in differently shaped macro-capsules saturated with phase change material. *J Energy Storage*. 2020;**31**:101635
28. Shin DH, Park J, Choi SH *et al*. A new type of heat storage system using the motion of phase change materials in an elliptical-shaped capsule. *Energy Convers Manag*. 2019;**182**:508–19
29. Vogel J, Felbinger J, Johnson M. Natural convection in high temperature flat plate latent heat thermal energy storage systems. *Appl Energy*. 2016;**184**:184–96
30. Huber C, Parmigiani A, Chopard B *et al*. Lattice Boltzmann model for melting with natural convection. *Int J Heat Fluid Flow*. 2008;**29**: 1469–80
31. Brent AD, Voller VR, Reid KJ. Enthalpy-porosity technique for modeling convection-diffusion phase-change—application to the melting of a pure metal. *Numer Heat Transf*. 1988;**13**: 297–318
32. Mbaye M, Bilgen E. Phase change process by natural convection-diffusion in rectangular enclosures. *Heat Mass Transf*. 2001;**37**: 35–42
33. Kamkari B, Shokouhmand H, Bruno F. Experimental investigation of the effect of inclination angle on convection-driven melting of phase change material in a rectangular enclosure. *Int J Heat Mass Transf*. 2014;**72**:186–200
34. Hong Y, Ye W-B, Huang S-M *et al*. Thermal storage characteristics for rectangular cavity with partially active walls. *Int J Heat Mass Transf*. 2018;**126**:683–702
35. Zhao JD, Zhai J, Lu YH, Liu N. Theory and experiment of contact melting of phase change materials in a rectangular cavity at different tilt angles. *Int J Heat Mass Transf*. 2018;**120**:241–9
36. Huang B, Yang S, Hu E, Li X, Wang J, Lund P Theoretical study on melting of phase change material by natural convection. *Case Stud Therm Eng*. 2021;**28**:101620
37. Arasu AV, Mujumdar AS. Numerical study on melting of paraffin wax with Al2O3 in a square enclosure. *Int J Heat Mass Transf*. 2012;**39**:8–16
38. Hosseini MM, Rahimi AB. Improving heat transfer in a triplex tube heat exchanger containing phase-change materials by modifications of length and position of fins. *Sci Iran*. 2020;**27**: 239–51
39. Dhaidan NS, Khodadadi JM, Al-Hattab TA *et al*. Experimental and numerical investigation of melting of NePCM inside an annular container under a constant heat flux including the effect of eccentricity. *Int J Heat Mass Transf*. 2013;**67**:455–68